J. Membrane Biol. 53, 63–75 (1980)

The Journal of
Membrane Biology

Decoupling of Heart Muscle Cells: Correlation with Increased Cytoplasmic Calcium Activity and with Changes of Nexus Ultrastructure

Gerhard Dahl* and Gerrit Isenberg**

I and II. Departments of Physiology, University of the Saarland, 6650 Homburg/Saar, West Germany

Summary. Purkinje fibers of the sheep heart were exposed to (a) 0.1 mM dihydro-ouabain (DHO), followed by (b) 0.1 mM DHO in Na-free solution or to (c) 1 mM dinitrophenol (DNP). The degree of electrical decoupling was characterized in terms of the inside longitudinal resistance r_i as measured with a 3-microelectrode voltage-clamp technique. Procedure *a* increased r_i by a factor of 3.7 ± 1.1 (mean $\pm$ SD), *b* by a factor of 9.8 ± 2.2, whereas in *c* incomplete voltage control indicated nearly complete uncoupling. Intracellular calcium activity (aCa_i) was monitored with a microelectrode system. At control conditions aCa_i was below 0.1 μM. The procedures listed above increased aCa_i to (a) 4 ± 1.5 μM, (b) 8 ± 2 μM, and (c) 36 ± 12 μM. The increase of aCa_i was in good correlation with the changes in core resistance. Effects on nexus ultrastructure, investigated with freeze-fracture techniques, are shown in histograms. At control conditions, the particle diameter distributed around a single peak (8.3 ± 0.5 nm). Procedures *b* and *c* induced a second population at 10.8 nm; increased decoupling reduced the control population in favor of the 10.8 nm population. Decoupling enlarged the width of the nexus gap by a factor of 1.6; again, the control population decreased in favor of a new population. In the decoupled state the heigth of the particle was smaller. Pits on the E-face displayed a more regular array and a nearly unchanged center-to-center spacing. Separation into several peaks was not possible due to scatter of the data.

We interpret the findings to mean that elevated aCa_i induces a conformational change of the nexus subunits which corresponds to a transition from an open to a closed state. The conformational change can be formally described by a particle contraction which disrupts the continuity with the particle of the adjacent membrane. Purkinje fibers exposed to DNP for 1 hr showed thinned (7.7 ± 0.5 mm) and elongated particles. We suggest that this is a secondary event and not a precursor of functional uncoupling.

Key words: Nexus, uncoupling, freeze fracture EM, intracellular calcium, heart.

Well-coordinated activity of individual muscle cells is an absolute requirement for the heart beat to be efficient for ejection of blood. This is achieved by electrical coupling of the cells, which has been found to be present in the heart muscle (Weidmann, 1952; Barr, Dewey & Berger, 1965) as well as between cells of a variety of excitable and inexcitable tissues (Loewenstein, 1966; Furshpan & Potter, 1968). Coupling of the cells combines them into functional units enabling passage of current and small molecules from one cell to another (*cf.* Loewenstein, 1975). A differentiated substructure in the area of cell contact is considered to provide a pathway for cell coupling. Such intercellular junctions are called nexus (Dewey & Barr, 1962) or gap junction (Revel, 1968) and have been shown to consist of an array of subunits (*cf.* McNutt & Weinstein, 1973; Casper et al., 1977).

The degree of cell coupling can be altered experimentally by hypertonicity (Barr et al., 1965) or by several treatments which commonly seem to result in a rise of the intracellular free Ca^{2+} concentration. The Ca^{2+}-hypothesis for the control of junctional permeability has been deduced from a series of studies on epithelial cells of *Chironomus* salivary glands (*cf.* Loewenstein, 1967, 1975; Rose & Loewenstein, 1976). While the validity of the Ca^{2+}-hypothesis for insect cells is based on a wide spectrum of experimental results (including measurements of cytoplasmic free

* *Present address:* Department of Physiology & Biophysics, University of Miami, School of Medicine, Miami, Florida 33101.

** Heisenberg fellow of the Deutsche Forschungsgemeinschaft.

0022-2631/80/0053-0063 $02.60

Ca^{2+}), there are only circumstantial evidences for its applicability to mammalian tissue. The latter are observations on injured heart cells (healing-over process, Délèze, 1970) and the uncoupling effect of Ca^{2+} injections into heart muscle cells (DeMello, 1975) and the effect of cyanide and iodoacetic acid on cultured cell lines (Flagg-Newton & Loewenstein, 1979). However, the validity of the Ca^{2+}-hypothesis for mammalian cells has also been doubted since Ca^{2+} translocation by ionophores had no effect on coupling of cultured heart cells (Gilula & Epstein, 1976).

Some attempts have been made to correlate uncoupling of cells and structural changes of the cell junctions, but with inconsistent results. Unfortunately, most of these studies have been performed on very different tissues. The aim of the present study was to investigate whether the degree of cell coupling, a change in intracellular free Ca^{2+} concentration, and structural aspects of the cell junctions are correlated with each other in one and the same preparation. For this purpose Purkinje fibers of sheep heart were used. The cells of these fibers are specialized for rapid conduction and are interconnected by nexuses which constitute 17% of the total surface plasma membrane (Mobley & Page, 1972). For their decoupling potency (Politoff, Socolar & Loewenstein, 1969; Rose & Loewenstein, 1976; Weingart, 1977) dinitrophenol (DNP) and cardioactive glycosides were applied. An intracellular Ca microelectrode, which is highly specific for Ca^{2+} (Oehme, Kessler & Simon, 1976), was used in order to follow putative changes in cytoplasmic calcium activity (aCa_i). Preparations with a known degree of decoupling and aCa_i subsequently were investigated with freeze-fracture electron microscopy. A preliminary report of these results has already appeared (Isenberg & Dahl, 1978).

Materials and Methods

Fine unbranched Purkinje fibers were obtained from hearts of freshly killed sheep. During the day of the experiments the fibers were stored at 32 °C in oxygenated Tyrode solution composed of 150 mM NaCl, 5.4 mM KCl, 3.6 mM $CaCl_2$, 1 mM $MgCl_2$, 10 mM glucose, buffered with HEPES-NaOH to pH 7.4. For the experiments a 2-mm long piece was pinned to the bottom of a small chamber (volume 0.1 ml) and superfused continuously (2 ml/min) with 37 °C warm Tyrode solution.

For intracellular recordings and stimulation we used bevelled microelectrodes with a tip resistance of about 3 MΩ (Isenberg, 1979). The clamp circuit controlling the membrane potential and the bath clamp measuring the corresponding membrane currents were described previously (Isenberg, 1977).

The degree of electrical decoupling was characterized by the relative change in the inside longitudinal resistance r_i^*/r_i, where r_i is the longitudinal resistance at control condition and r_i^* that of fibers subjected to decoupling procedures. To calculate r_i^*/r_i (as shown in Fig. 1) the following assumptions should be satisfied:

1) Application of the cable equations (Adrian, Chandler & Hodgkin, 1970; Jack, Noble & Tsien, 1975) requires that the membrane resistance r_m and the longitudinal resistance r_i are continuously distributed parameters. The observation of a part of nexus particles undergoing ultrastructural changes, however, suggests that a model described a network of discrete resistances might be necessary to avoid erroneous estimates of r_i^*. Calculations where a continuous and a discrete model are compared have shown, instead, that significant descrepancy only arises with the length constant λ equalling the cell length h (Socolar & Loewenstein, 1979). Since within the chosen margins $r_i^*/r_i \leqq 10 - \lambda$ exceeded h by a factor of 4, the underestimation of r_i^* is negligible. Furthermore, inserting electrode B at various distances X (smaller than the cell length) to C in partially uncoupled fibers resulted in voltage deflections ΔV changing continuously with X.

2) Factor p (Adrian et al., 1970), correcting for nonlinearities of the cable equations, should deviate from 1 by not more than 5%. As, e.g., DHO reduces r_m by a factor of 4 (*see* page 66), the 5% error limit is not exceeded as long as r_i^*/r_i is below 9. For greater quotients (DNP experiments) quantitation becomes impossible.

3) Decoupling should not modify the core diameter (d in Fig. 1) or the electrode spacing a. The stability of d and a were controlled with the light microscope. That d and a remained constant despite the mechanical contracture may be a peculiarity of sheep Purkinje fibers, which have only a poorly developed contractile aparatus (Caesar, Edwards & Ruska, 1958).

Estimation of the Intracellular Calcium Activity aCa_i

Calcium sensitive microelectrodes were fabricated by filling siliconized (Lux & Neher, 1973) bevelled tips (Isenberg, 1979) with the Simon-type calcium carrier N,N′-di(11-ethoxycarbonyl) undecyl-N,N′, 4,5-tetramethyl-3,6 dioxaoctane diacid amide (*compare* Oehme et al., 1976). They had resistances between 5 and 15 GΩ; when referred to a bevelled 3-M KCl microelectrode they exhibited a noise level of 0.3 mV and a drift of less than 1 mV per hr.

The calcium-sensitive microelectrode system was calibrated in an activity scale using a Ca-ion activity coefficient of 0.31 for Tyrode solution (calculated from the Debye-Huckel theory with the Guggenheim convention; *compare* Bates, 1973; Blaustein, 1974; Meier et al., 1977). Thus, Tyrode solution containing 3.6 mM $CaCl_2$ has an activity of 1.1 mM. Calibration standards were obtained by diluting this Tyrode solution with nominally Ca-free Tyrode solution (contaminated with ~0.5 μM Ca^{2+}). The calcium-sensitive system showed a Nernst response between $aCa = 10^{-3}$ and 10^{-6} M; the slope factor s was between 26 and 29 mV. When 2 mM EGTA was added to the nominally Ca-free Tyrode solution, V_{Ca} decreased from −90 to approximately −120 mV. The latter value indicates that the lowest aCa detectable is in the order of 50 nM (*compare* Simon et al., 1978). Calibration with Ca-EGTA standards was not applied due to the controversy about the Ca-EGTA association constant. The calibrated V_{Ca} signals include contributions of the reference electrode's liquid junction potential (tip potential), which may change when the reference electrode is inserted into the cell. This situation was simulated by substituting NaCl by KCl (150 mM) in the Tyrode solution. Since this changed V_{Ca} by +1 to +2 mV only, the influence of the liquid junction potential was ignored. Actual intracellular measurements are shown in Fig. 2.

From measurements on 20 Purkinje fibers giving $V_{Ca} = 112 \pm 6.5$ mV, we calculated aCa_i to be 83 ± 15 nM (mean ± SD).

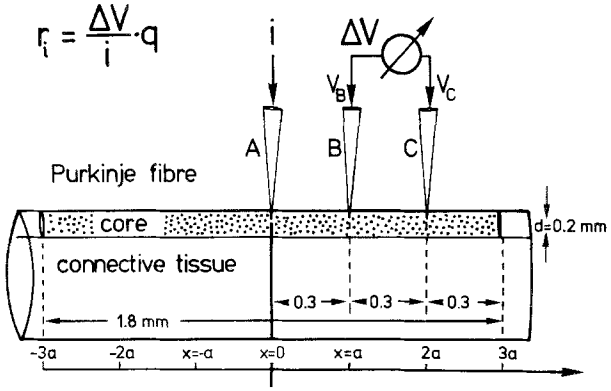

Fig. 1. Arrangement for measuring the inside longitudinal resistance r_i. A Purkinje fiber 2 mm in length contains about 200 excitable cells in its core, each of them 50 μm in diameter and 125 μm in length (mean values). As 3 microelectrodes were impaled at a distance of $a=0.3$ mm, at least one cell-to-cell junction should be between any two neighboring tips. The cable equations (Adrian et al., 1970; Jack et al., 1975) predict that the ratio of the modified longitudinal resistance r_i^* over the resitance r_i measured at control conditions is given by $\frac{r_i^*}{r_i} = \frac{\Delta V^*/i^*}{\Delta V/i}$ (for restrictions, *see* text). In most of the experiments electrode *B* was filled with a calcium carrier-resin (Oehme, Kessler & Simon, 1976). When electrode *A* did not inject current, the difference $V_c - V_B$ indicated the intracellular calcium activity $a\mathrm{Ca}_i$

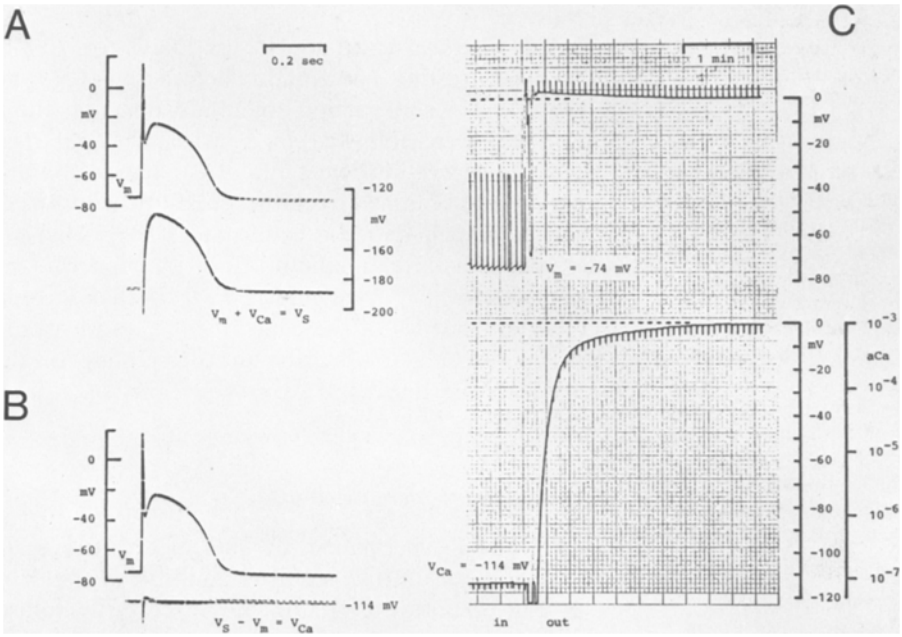

Fig. 2. Estimation of the intracellular calcium activity by means of a Ca-sensitive microelectrode system. (*A*): Impalement by the Ca electrode delivers a signal V_s, which is composed of the membrane potential V_m (including the action potential) and the signal V_{Ca} due to the Ca gradient across the membrane. The action potential recorded with the Ca-sensitive tip does not show the high frequency components such as the overshoot, but the plateau potential is identical to that recorded with the conventional electrode. The latter finding indicates that electrodes *A*, *B* and *C* (Fig. 1) are inside the same core. (*B*): The record in the differential mode gives $V_{Ca} = V_s - V_m = -114$ mV. V_{Ca} is almost constant during the action potential, due to the short electrical but long chemical response time of the Ca-sensitive tip. (*C*): Withdrawal of the tips is followed by a jump in the membrane potential ($V_m = -74$ mV; upper trace recorded with the reference electrode) and a slowly responding Ca signal (lower trace). One calculates from $V_{Ca} = -114$ mV and $a\mathrm{Ca}_o = 1.1$ mM (concentration 3.6 mM) an $a\mathrm{Ca}_i = 92$ nM. The true $a\mathrm{Ca}_i$ might be lower, since interference by $a\mathrm{K}_i$ restricts the Ca electrode's response

However, one has to interpret this value as an upper limit for the resting $a\mathrm{Ca}_i$; since the Nernst slope factor *s* declines at activities close to the detection threshold, the true $a\mathrm{Ca}_i$ value may be much lower than 83 nM.

Finally, it should be noted that any increment in $a\mathrm{Ca}_i$ will be indicated with a time lag due to the rather long response time. Furthermore, any increase of $a\mathrm{Ca}_i$ may have to exceed a threshold for detectability. Also, one should bear in mind that the Ca-sensitive tip sees $a\mathrm{Ca}_i$ within the cytosol but not immediately at the nexus membrane. Due to the nonconstant slope a quantitative calculation from V_{Ca} to $a\mathrm{Ca}_i$ is difficult for $a\mathrm{Ca}_i < 1$ μM. For greater activities, however, interpretation should be unique and the selectivity of Ca over Mg or K and Na appears to be perfect (*see* Simon et al., 1978).

Some of the experimental conditions (e.g., exposure to high doses of dihydro-ouabain) made the fibers' membrane potential oscillate between −35 and −65 mV (*compare* Ferrier, Saunders & Mendez, 1973). Since the fiber conducts these oscillations with low speed, the membrane potential at point *B* may deviate from that of point *C*. This kind of error was reduced by averaging the signals V_s (*B*) and V_m (*C*) graphically before V_{Ca} was obtained by subtraction.

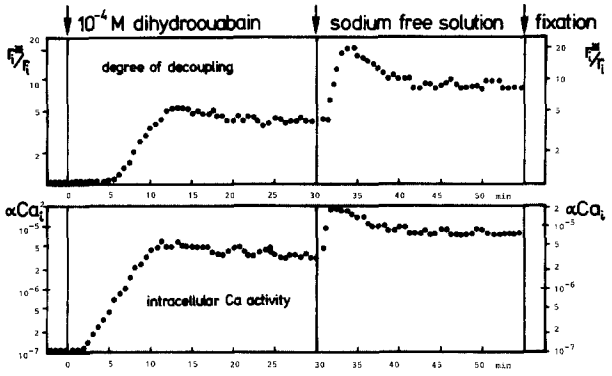

Fig. 3. A toxic dose of dihydro-ouabain increased the inside longitudinal resistance to 5 times the control value, which indicates a considerable degree of decoupling (upper panel). It enhances the intracellular calcium activity from less than 0.1 to about 5 μM (aCa_i in logarithmic scale, lower panel). Then superfusion with a DHO-containing sodium-free Tyrode solution evoked a further increase in aCa_i and further decoupled the cells. One hour after the first exposure to DHO the electrical measurements ended and the preparation was fixed (arrow) for electronmicroscopy. To estimate r_i^*/r_i the preparation was clamped every 8 sec (duration <2 sec); every dot represents mean values calculated from 5 clamp steps. During the current-free periods the calcium signals were obtained; the dots represent the mean of 5 tracings (each of 6 sec duration)

Electron Microscopy

Purkinje fibers, in which the decoupling of the cells had been characterized by the increased ratio r_i^*/r_i and the concommittant increment in aCa_i had been measured, were fixed at 37 °C by replacing the superfusing Tyrode solution by a solution composed of glutaraldehyde (2%), Na-cacodylate buffer (80 mM), and $CaCl_2$ (2 mM). (The osmotic pressure of the solution was adjusted to 370 mosmol.)

After 1 hr of fixation the specimens were immersed in 30% glycerol for 30 min. Freeze-fracturing was performed according to standard techniques in a Balzers BAF 300 unit equipped with an electron beam gun for platinum-carbon (45°) and carbon evaporation and with a thin-film monitor measuring the thickness of the evaporated material. All preparations were performed at a vacuum of 6×10^{-7} Torr, and a specimen stage temperature of −100 °C; and Pt/C shadowing (20 Å) was started immediately after fracturing.

Electron photomicrographs were obtained on a Siemens Elmiskop 101. Measurements were performed on micrographs enlarged to 300,000×.

All measurements are uncorrected for the thickness of an adsorption layer and of the shadowing material. Denomination of the membrane fracture faces follows the convention of Branton et al. (1975).

Results

Electrical Decoupling by Dihydro-Ouabain

It has previosly been shown that the inside longitudinal resistance r_i of ventricular muscle preparations increased by a factor of 3, when they were exposed to a toxic dose of ouabain (2×10^{-6} M) for 3 hr (Weingart, 1977). For decoupling of Purkinje fibers we used instead the derivative dihydro-ouabain (DHO) for its faster effectiveness (Isenberg & Trautwein, 1974; Deltmer & Ellis, 1978), in a concentration of 10^{-4} M (corresponding to about 5×10^{-6} M ouabain).

Figure 3 (top) shows the decoupling effect of DHO in terms of the ratio r_i^*/r_i. Initially, there was a period of about 5 min without any change. Following this delay, r_i^*/r_i increased within 8 min by a factor of 5. The increase displayed a nearly exponential time course (time constant 150 sec). With further exposure to DHO r_i^*/r_i declined again and became stable at a value of 4.

The fibers exposed to 10^{-4} M DHO for 30 min displayed resting potentials between −65 and −76 mV. The short action potentials (duration about 150 msec) were followed by "transient depolarizations" (*compare* Ferrier et al., 1973). The membrane resistance r_m obtained from the slope of the hyperpolarizing branch of the steady-state *i-V* relationship declined to as little as about 1/3 of the control. One calculates from $r_i^*/r_i \geqq 5$ and $r_m^*/r_m \leqq 1/3$ that λ could fall as far as to 1/4 of the control value, and it would still be possible to describe the decoupling of the cells with the linearized cable equations of Adrian et al. (1970).

Concommitant Increase in aCa_i

In the DHO experiments, no sign of an increase in aCa_i appeared until 90 sec after addition of the drug (*see* Fig. 3, bottom). It does not necessarily follow that aCa_i remained constant during this delay; since the threshold for the electrode response is about 0.1 μM (*see* p. 64), another interpretation could be that aCa_i increased from a resting activity of around 10^{-8} to 10^{-7} M during this period of 90 sec. When, after 5 min, the first decoupling effect was seen, aCa_i nominally was 0.5 μM. The maximum aCa_i was reached about 10 min after administration of DHO, i.e., 1 to 2 min earlier than r_i^*/r_i peaked. Nevertheless, the increase of both parameters is strongly correlated; both time constants are identical. Furthermore, longer exposure to DHO reduces both aCa_i and r_i^*/r_i.

Further Decoupling and Increment in aCa_i by Sodium Removal

According to the hypothesis that blocking the sodium pump (by DHO) primarily increases the intracellular

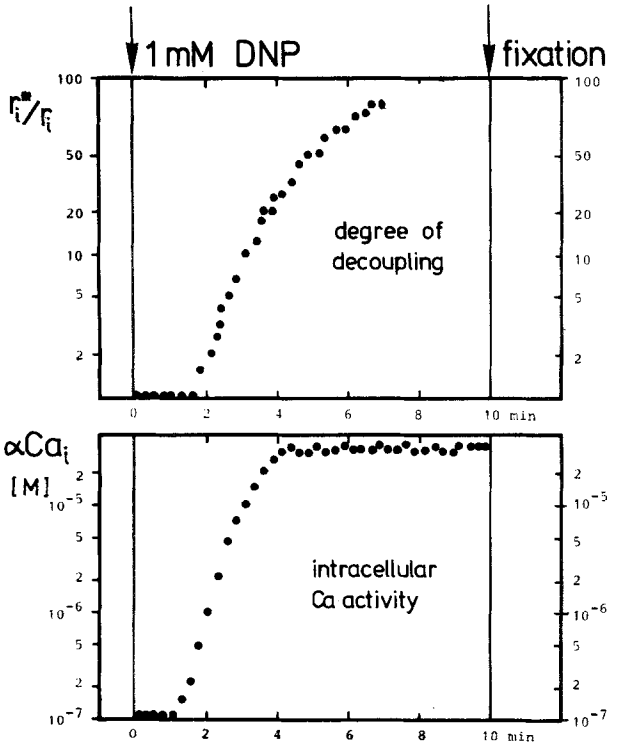

Fig. 4. 2,4-dinitrophenol (1 mM) increased aCa_i rapidly to a steady level of 40 μM. With a delay, decoupling developed. After an exposure of 8 min, measurements of resistance ended, since the clamp circuit could no longer control the fibers' membrane potential

sodium content, to which aCa_i is related via the Na-Ca-exchange mechanism (Reuter & Seitz, 1968; Langer & Serena, 1970), one expects a further gain in aCa_i when the Na gradient is reversed by a sodium-free Tyrode solution.

As expected, substitution of 150 mM NaCl by 150 tetramethylammonium chloride (TMA) enlarged aCa_i appreciably. The electrode indicates a maximum aCa_i (20 μM) at 2 min after changing of the perfusate. Within the following 15 min, aCa_i declined; the steady level was about 7 μM.

The degree of decoupling as measured by r_i^*/r_i (Fig. 3, top right) followed the changes in aCa_i with a delay of about 1 min. Three min after a change to the Na-free perfusate, r_i^*/r_i reached a maximum of 20; afterwards it fell to a steady value of 9. Despite the delay of 1 min, the changes in aCa_i and r_i^*/r_i are closely correlated.

The sodium-free perfusate increased the membrane resistance by a factor of 1.2. Although the space constant $\lambda^* = \sqrt{r_m^*/r_i^*}$ amounted to only 1/5 of the control, it was still greater than the interelectrode distance. Hence r_i^*/r_i can be evaluated by the method proposed.

Mean Values

The procedures illustrated in Fig. 3 were applied altogether to 7 preparations. A 30-min treatment with 10^{-4} M DHO induced an increase of $r_i^*/r_i = 3.7 \pm 1.1$ (mean ± SD). The corresponding aCa_i amounted to 4 (±1.5) μM. During the following superfusion with sodium-free solution, r_i^*/r_i had a steady value of 9.8 ± 2.2; aCa_i was found to be 8 ± 2 μM.

Experiments with DNP

In order to increase cytoplasmic calcium activity by a different mechanism we applied DNP, which may also have a more pronounced decoupling effect (Politoff et al., 1969; Rose & Loewenstein, 1976).

For the experiment illustrated in Fig. 4, DNP was applied in a concentration of 1 mM. After a 1-min latent period (*compare* with the latency in Fig. 3) the signal of the Ca-sensitive electrode rapidly exceeds the 0.1 μM threshold. Four min after application of DNP, aCa_i reached a steady level of 40 μM.

The time course of decoupling resembled that of the increment in aCa_i. Seven min after application of DNP, r_i^* was 80-fold larger than the control value r_i. Afterwards, the voltage-clamp circuit could no longer adequately control the potential of the electrode C, suggesting a great degree of decoupling which cannot be quantified. Despite this general agreement, r_i^*/r_i behaved differently from aCa_i in detail. Not only did aCa_i have to increase beyond 4 μM before any change in r_i^*/r_i was measured, but, furthermore, the uncoupling effect became steady much later than aCa_i.

The effect of 1 mM DNP was investigated in 6 preparations, all of which showed the tremendous increase in aCa_i described above. In the steady state aCa_i was between 20 and 55 μM; the mean for the 6 fibers was 36 ± 12 μM. The time course of cytoplasmic calcium accumulation varied: when DNP was applied to a "fresh" fiber (the animal being killed no longer than 3 hr before), aCa_i needed 20–30 min to reach a 10 μM level, whereas fibers stored in the laboratory for 10 hr gained calcium as fast as shown in Fig. 4.

All fibers displayed a high degree of decoupling, the final r_i^*/r_i ratio always exceeding 80. In fibers the potential V_c could not be affected at all (complete uncoupling). Voltage control was inadequate for evaluating the membrane resistance. The resting potentials ranged between −35 and −25 mV.

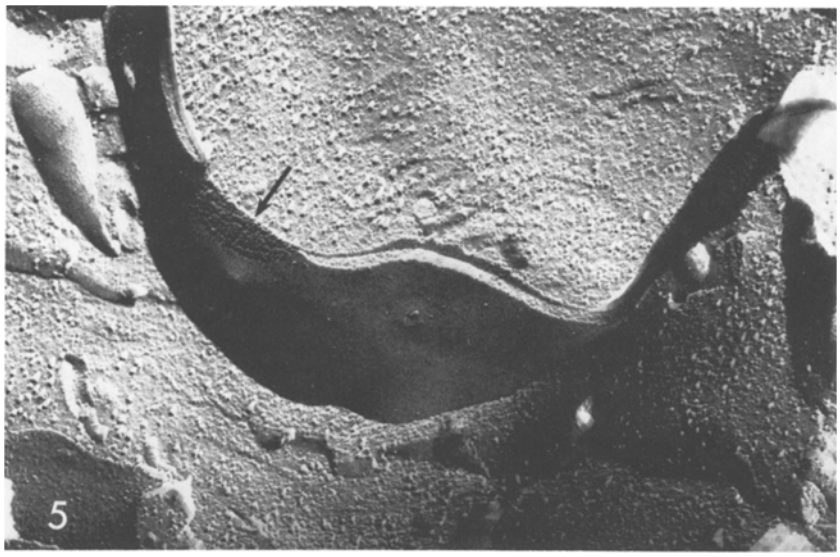

Fig. 5. Freeze-fracture electronmicrograph of a sheep Purkinje fiber at control conditions. Nexus is shown in partial transverse fracture (arrow). Magnification, 54,000 ×

Nexus Ultrastructure at Control Conditions

The ultrastructural substrate of the low-resistance pathway between myocardial and other cells is considered to be represented by the nexus (gap junction) (reviewed by McNutt & Weinstein, 1973). In Purkinje fibers nexuses are not found preferentially at the intercalated discs as in ventricular muscle, but they occur all over the cell surface. Nexuses (Fig. 5) are close appositions of cell membranes where a densely-spaced array of membrane-associated particles with uniform dimensions is visible on the protoplasmic leaflet of the cell membrane (*P*-face) and corresponding pits appear on the exoplasmic leaflet (*E*-face) of freeze-fractured cells.

The following parameters have been quantitatively evaluated in order to follow putative morphological changes of nexuses resulting from uncoupling procedures: center-to-center spacing, order of array, and diameter of the subunits. These are the parameters usually used to characterize nexus morphology. However, while these parameters are commonly measured on nexus particles, in order to minimize sources of error we preferred measuring center-to-center spacing and order of array on pits since particles can be subject to some plastic deformation during the freeze-fracture process. In addition, the height of particles and the relative width of the nexal gap have been determined.

A nexus of a Purkinje fiber with low longitudinal resistance and intracellular Ca activity $\leqq 10^{-7}$ M is shown in Fig. 6. The measurements of ultrastructural parameters in such control preparations are presented as histograms in Fig. 7.

The *diameter of the particles* was measured perpendicularly to the direction of shadowing. Around a mean of 8.3 nm the values are distributed nearly symmetrically between 7 and 10 (SD $= \pm 0.5$ nm). The *height of the particles* can be determined from the shadow length which, when multiplied by the tangent of the angle of shadowing, equals the height of the shadowed prominence. While the angle of the shadowing source was fixed at 45° to the general fracture plane, the actual path of cleavage meanders and will introduce errors in the angle of shadowing. The histogram of the frequency of heights, therefore, lies within the broad range from 3 and 17 nm; the mean corresponds with the distribution's maximum, 9 ± 2.4 nm. (The numbers given for the particles' diameter and height are uncorrected for errors due to the replication method.)

We have characterized the gap between adjacent membranes in a nexal area by the length of the shadow projected from the surface of the membrane *E*-face onto the (top) of the *P*-face particles. To reduce the errors introduced by the deviation of the actual fracture plane, this shadow length has been devided by the shadow length of adjacent particles. These normalized data are shown as *relative width of the gap* (Fig. 7). They are distributed around a mean of 1.17 ± 0.21; this would be equivalent to a distance of 10.5 ± 2 nm between the surface of the *E*-face and the top of the *P*-face particles. (Again, this value is uncorrected for the material deposited with the replication method.)

For the *center-to-center spacing* of the nexus subunits the distance between neighboring pits (membrane *E*-face) has been measured. The nearly symmetric histo-

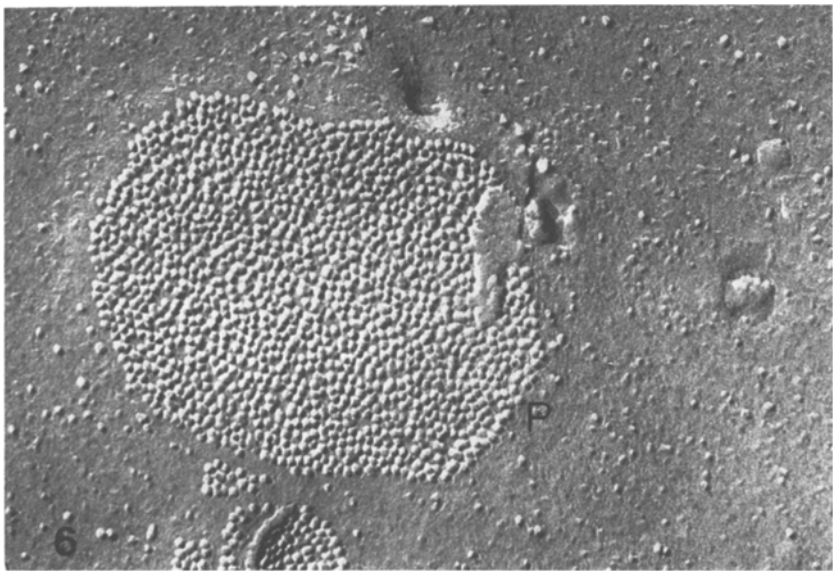

Fig. 6. Freeze-fracture EM revealing the nexus array at control conditions. It displays the cytoplasmic leaflet (*P*-face) which is studded with nexus particles. Magnification, 135,000 ×

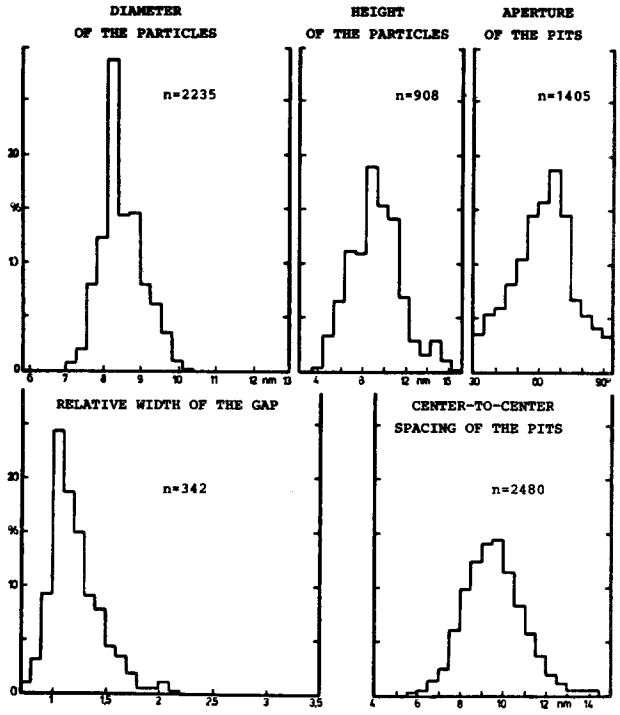

Fig. 7. Histograms characterizing the nexus ultrastructure at control conditions

gram is distributed between 4 and 10 nm and displays a mean of 9.4 ± 2 nm. The *aperture of the pits* characterizes the regularity of the array. If the array would be a regular hexagon, the histogram should display angles of 60° only; the broad distribution (SD = 15.3°) seen in Fig. 7 indicates that at control conditions regularity is not well expressed.

Changes in Nexus Ultrastructure Observed in Decoupled Preparations

Nexus parameters from Purkinje fibers treated for 30 min with 10^{-4} M DHO and for another 30 min with *Na-free solution* are illustrated in Figs. 8 and 9. The histogram of the particle diameter shows the most obvious changes; on the average, the particle is thickened from 8.3 to 9.1 nm. Furthermore, the values no longer fall symmetrically around a single mean. Instead, one may classify the data around two peaks ($\bar{x}_1 = 8.2$ nm; $\bar{x}_2 = 9.6$ nm); an interpretation with more than two peaks (e.g., $\bar{x}_1 = 8.2 \pm 0.3$ nm; $\bar{x}_2 = 9.6 \pm 0.4$ nm; $\bar{x}_3 = 10.8 \pm 0.6$ nm), of course, is also possible. The histogram of the particle height indicates a small shrinkage, from 9 to 8.5 ± 0.2 nm (significance with $P = 0.2$); no separation into several peaks is obvious, due to the great scattering of the data. Two peaks can be seen again in the histogram of the relative width of the gap; the data (obtained from normalized shadow length) distribute around $\bar{x}_i = 1.1 \pm 0.2$ nm and $\bar{x}_2 = 2.0 \pm 0.4$ nm. In the mean the relative width of the gap increased from 1.1 to 1.59. Per definition (*see* p. 68) this statement is based on the assumption of an unaltered particle height, the latter changed, but, to a degree (5%) which cannot account for the increased relative width of the gap. The nexus *E*-face subunits are arranged with more regularity (dominance of aperture angles close to 60°, indicated by a SD of 8.7° only) and seem to be more aggregated, as indicated by reduction of the center-to-center spacing from 9.4 ± 2 nm to 9.1 ± 1.8 nm ($P = 0.2$).

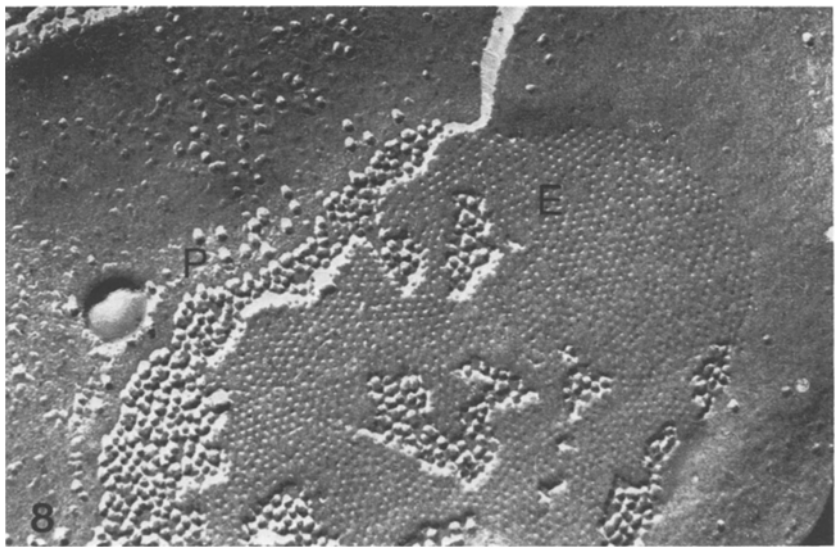

Fig. 8. Ultrastructure of a nexus from a preparation partially decoupled with DHO poisoning and following Na removal. Particles on the *P*-face and pits on the *E*-face are more regularly arranged. Magnification, 135,000×

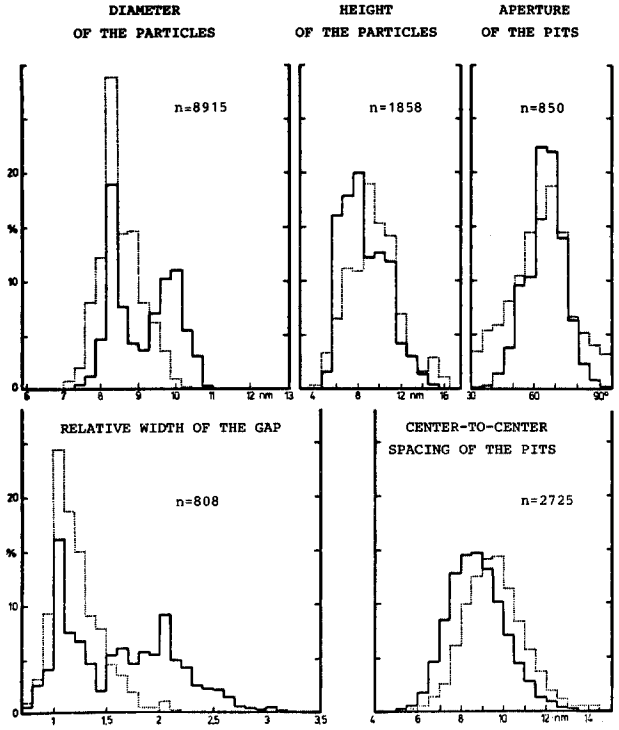

Fig. 9. Histograms characterizing the nexus ultrastructure of preparations in a partially decoupled state. The Purkinje fibers were treated for 30 min with 10^{-4} M DHO and for another 30 min superfused with a Na-free (DHO containing) Tyrode solution. For comparison, the histograms of the control state are shown by dotted lines

The nexus parameters of Purkinje fibers treated for *15 min with DNP* (Fig. 10, histograms of Fig. 11) show the same kind of ultrastructural changes as found in response to DHO. As expected from the greater degree of uncoupling (and the high Ca activity of about 50 μM), the changes in ultrastructure were more pronounced: concerning mean values, the nexus particles thickened in their diameter (9.8 instead of 8.2 nm at control) and shrank in their height (8 instead of 9 nm), the relative width of the gap extended (from 1.1 at control to 2.1). Figure 11 shows that the particle diameters group clearly around two peaks, the percentage of the control distribution ($\bar{x}_1 = 8.1 \pm 0.3$) being reduced to 27% in favor of the second population, peaking at $\bar{x}_2 = 10.8 \pm 0.6$ nm. In a similar way one may interpret the histogram concerning the relative width of the gap: the population around $\bar{x}_1 = 1.1 \pm 0.16$ declined to 8.5% of the total, the majority being distributed around $\bar{x}_2 = 2.1 \pm 0.44$.

Regarding the *E*-face subunits, the center-to-center spacing remained almost unaltered (9.5 ± 2.2 nm instead of 9.4 ± 2.0 nm at control conditions). Figure 11 shows that the subunits are more regularly arranged (aperture of the pits distributed with a SD of $\pm 10.5°$).

An interpretation of the ultrastructural changes paralleling decoupling and increased intracellular calcium activity is proposed as follows:

Increased intracellular Ca activity induces a conformational change of the subunits. This change reduces the height and increases the diameter of the particles, which is comparable to a contraction. Such a contraction may not disturb the fixation of the particle within its "own" membrane but it may disrupt the alignment between particles of the 2 different, adjacent membranes, thereby splitting the nexus halves and increasing the relative width of the gap. The larger particle diameter could promote the interactions between adjacent subunits of the same membrane, thus inducing an increased regularity in the array. The conformational changes could have closed the hemi-channels and disrupted their continuity.

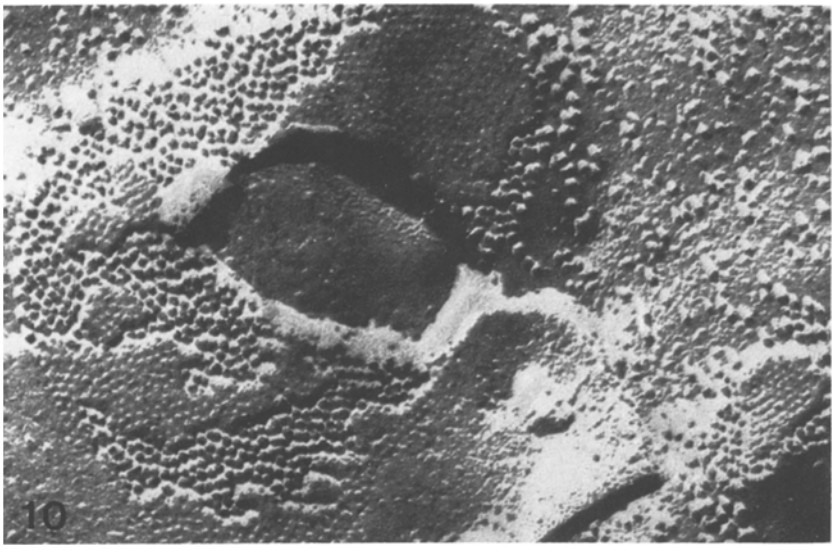

Fig. 10. Ultrastructure of a nexus from a preparation strongly decoupled with 1 mM DNP (15 min). Magnification, 135,000×

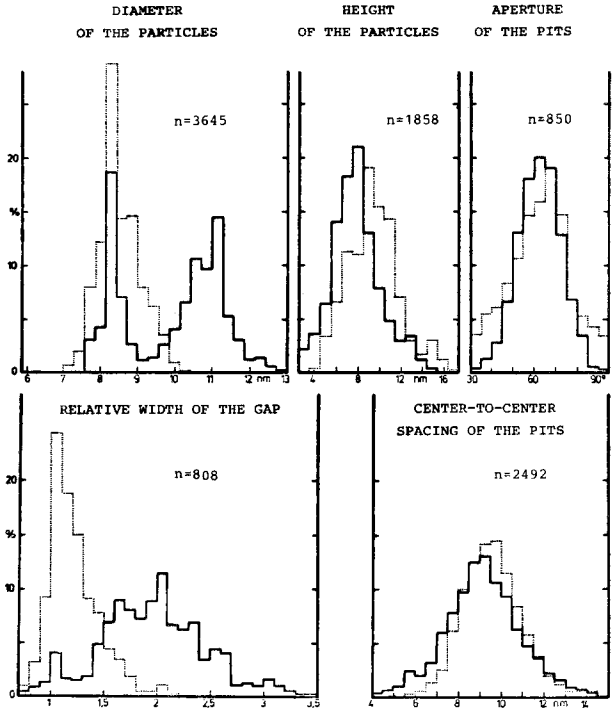

Fig. 11. Histograms characterizing the nexus ultrastructure of preparations in a strongly decoupled state. The fibers were exposed to 1 mM DNP over a period of time (mean 15 min) sufficient to increase r_i^*/r_i to more than 80. For comparison, the histograms of the control state are shown by dotted lines

Nexus Ultrastructure in Purkinje Fibers Treated with DNP for 1 hr

The ultrastructural changes described above are different from those reported for the nexus of septal giant axons (Peracchia & Dulhunty, 1976) or stomach epithelial and liver cells (Peracchia, 1977) where it has been reported that uncoupling evoked by DNP (0.5 to 5 mM) reduces the particle's diameter (instead of increasing it) and narrows the center-to-center spacing. But, before fixation Peracchia exposed his preparations to DNP for 1–2 hr whereas we fixed the fibers after 15 min. In order to test whether this difference in time could account for the discrepancy, we investigated the nexus ultrastructure of Purkinje fibers treated with 1 mM DNP for 1 hr (Figs. 12 and 13).

The nexus particles seen in these preparations have a smaller diameter (7.7 ± 0.5 nm) and a greater height (8.6 ± 2.4 nm) as compared to the control. The values of the particle diameter are distributed around a single peak. So, this histogram differs clearly from that obtained for fibers treated with DNP for only 15 min (dotted line for comparison). The histograms of the pits of the *E*-face indicate that the subunits have aggregated (center-to-center spacing reduced to 9.0 ± 1.7) and are highly ordered; the aperture of the pits is distributed with a SD of 8.2° around an increased maximum at 60°.

These data suggest that nexal subunits may undergo a complex sequence of changes in response to uncoupling procedures. The morphological changes observed in the shorter time scale (DNP for 15 min) are more likely to be a reflection of the uncoupling process than those observed in specimens where uncoupling has already persisted some time (DNP for 1 hr). The latter may indicate that under these conditions a degradation of nexuses already takes place.

Discussion

From the present results, it appears that *the Ca^{2+}-hypothesis of control of cell-cell coupling* (Loewenstein,

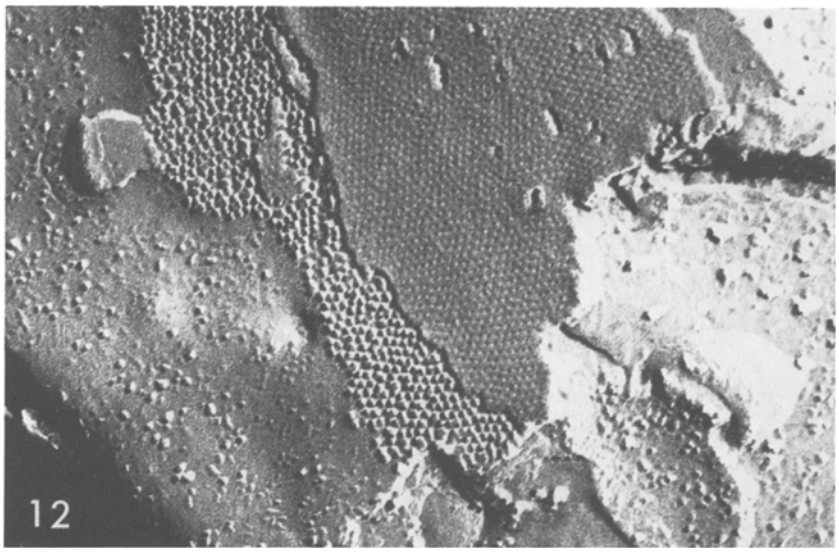

Fig. 12. Ultrastructure of a nexus from a preparation treated with 1 mM DNP for 1 hr. Magnification 135,000×

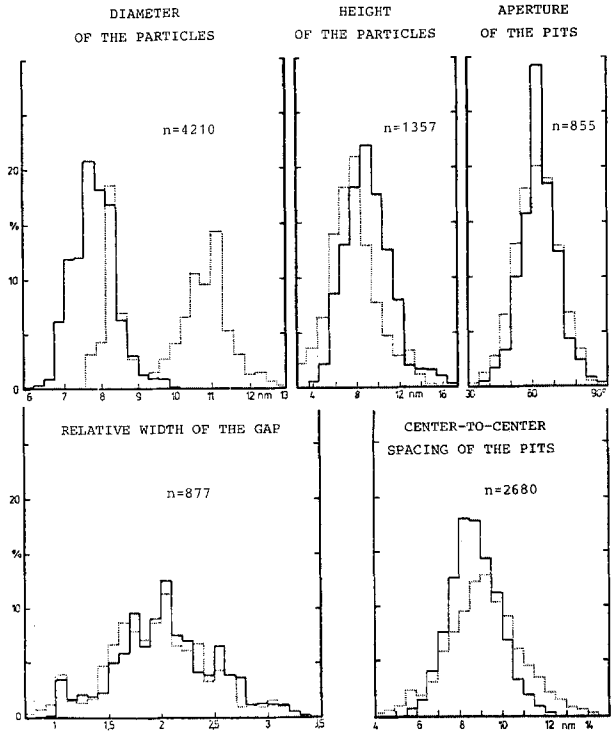

Fig. 13. Histograms characterizing the nexus ultrastructure of preparations treated with 1 mM DNP for 1 hr. For comparison, the histographs of preparations treated with 1 mM DNP for 15 min are shown by dotted lines

1975), originally developed in relation to insect cells, is valid for mammalian tissue as well: the uncoupling procedures increased aCa_i in parallel with the development of decoupling, and the changes in nexus ultrastructure followed. DHO (or DHO and sodium-removal) and DNP increase aCa_i via different mechanisms (Na-Ca exchange at the cell membrane; Ca-release from mitochondria), suggesting that the elevated aCa_i can be considered to be a causal and not simply a coincidental event for the decoupling process.

The procedures used in this study should have elevated aCa_i in all the cells of the Purkinje fibers' core by the same degree, resulting in a symmetrical rise of aCa_i on both cytoplasmic sides of the junction. But, the increase in aCa_i might not be totally uniform; mitochondria and vesicular membrane structures (similar to those of the sarcoplasmic reticulum) can often be found in the neighborhood of the nexus (*see* Fig. 14), and their activity could effectively control the calcium activity of the cytoplasmic nexus surface. In normal, Ca-balanced cells this control mechanism is sufficient to avoid decoupling during contraction (aCa_i about 3 μM), but a general long lasting calcium rise might overload this sequestering system. Finally, these organelles could release calcium-ions instead of picking them up. Because inhomogeneity of aCa_i distribution could thus result, we cannot consider the aCa_i of 0.5 μM (Figs. 3 and 4) as the "true threshold aCa_i" for the first measurable decoupling effect, and the parallel onset of changes in aCa_i (logarithmic scale) and r_i^*/r_i might be a fortuitous event. However, the order of magnitude of the rise in aCa_i during the progress of uncoupling (to aCa_i about 50 μM) is in fairly good agreement with data found with aequorin signals (Rose & Loewenstein, 1976) in the salivary gland of *Chironomus*.

Studies on nexus formation in reaggregated cells revealed a quantal increase in junctional conductance in nascent junctions, indicating that junctions are formed of multiples of identical units (Loewenstein,

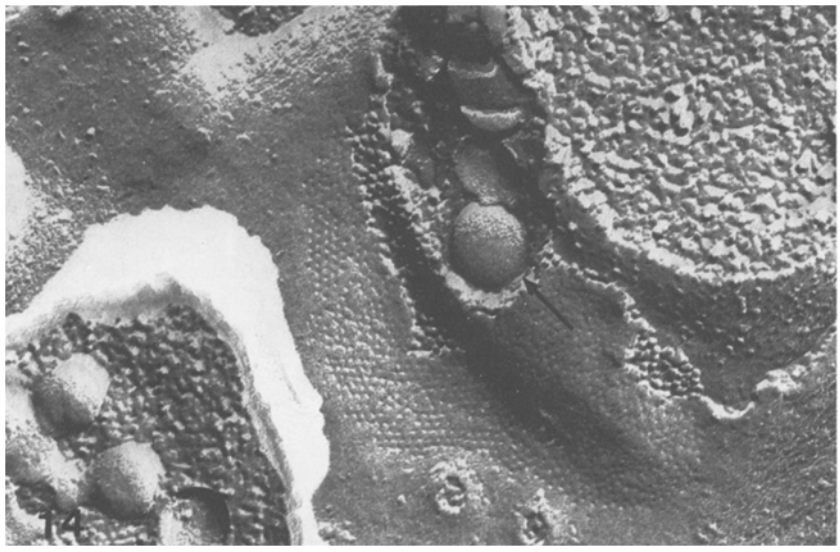

Fig. 14. Vesicular structures (arrow) similar to the sarcoplasmic reticulum might be considered to control calcium activity at the cytoplasmic side of the nexus membrane

Kanno & Socolar, 1978). According to the present knowledge of the junction morphology, it can be assumed that each intramembraneous particle seen in freeze-fractured junctions represents a hemichannel. A gradual impairment of cell-cell transmission in response to a rise of cytoplasmic [Ca^{2+}] could be due either to (a) a uniform gradual diminution of the channel size or (b) a reduction in number of open channels by an all-or-none closure of channels. Studies following the cell-cell transfer of tracer substances which are smaller but close to the size of channels in untreated junctions have been interpreted as showing a graded exclusion of tracer substances according to their size or an all-or-none closure of an inhomogenous population of channels in response to a rise of cytoplasmic [Ca^{2+}] in salivary glands of *Chironomus* (Rose, Simpson & Loewenstein, 1977). Conductance measurements of single channels in nascent junctions did not solve the problem. Injection of Ca^{2+} intracellularly has been reported to reverse the channel accretion in reaggregated cells in quantal steps which in some cases have been of the same magnitude as those observed during formation of the channels. On the other hand, some of the voltage step decrements differed in magnitude suggesting a partial closure of the channels (Loewenstein et al., 1978). The increase in core resistance of Purkinje fibers by DHO and DNP observed in the present study could be explained in both ways. Provided that the morphological changes observed in DNP-treated fibers (15 min) reflect the change in junctional state of the channels, these data, however, would favor the hypothesis of an all-or-none closure of the channels. An increasing degree of uncoupling was not accompanied by graded changes of particle size, but, instead, the fraction of particles in the control state declined, while a different population of particles appeared. This assumes that broadening of the peak is due to errors of measurement. Unfortunately, the electrical data do not tell whether the cells are completely uncoupled or whether there are still some cell-cell channels in the open state which would account for the persistence of particles in the control group.

Several studies have tried to correlate the different functional states of the cell-cell channels with changes in ultrastructure of the nexuses. The reports on morphological changes in response to other uncoupling procedures, which mostly seem to share an elevation of cytoplasmic [Ca^{2+}], are inconsistent. Based on thin-section EM studies, in uncoupled cells the width of the gap between cell membranes within the junctional area has been reported either to be increased – in some studies nexuses could not further be identified with this method (Asada & Bennett, 1971; Pappas, Asada & Bennett, 1971; McCallister, Munger & Neely, 1977; Volkmer et al., 1977), to be unchanged (Ashraf & Halverson, 1978) or to be decreased (Peracchia & Dulhunty, 1976). The decrease of the junctional thickness found in thin sections, however, was not confirmed by optical diffraction methods (Peracchia, 1977).

In the present study with the freeze-fracture technique, the relative width of the gap (*see* definition above), which comprises the actual gap, has been found to be increased in uncoupled Purkinje fibers as compared to control. A more detailed analysis of nexus structure in freeze-fractured Purkinje fibers confirmed the earlier description of morphological changes found in liver and stomach epithelial tissues

subjected to hypoxia and treated with DNP, which both were assumed to result in uncoupling of these cells (Peracchia, 1977). However, this holds only for those data which have been obtained under comparable conditions of uncoupling procedures (DNP for 1 hr). By contrast, different changes have been found in Purkinje fibers processed for EM after a shorter time of incubation with DNP, despite a comparable degree of decoupling. It is tempting to assume that the earlier morphological changes are much more likely to reflect changes in functional state of nexuses than the subsequent ones, which might already be an indication of nexus degradation.

The necessity of chemical fixation of the tissue for EM processing is a handicap: fixation with glutaraldehyde, the most common fixative, has been shown to have an uncoupling effect by itself (Bennett, 1973). Whether this is a Ca^{2+}-mediated phenomenon or a direct action of glutaraldehyde on nexuses is unclear. While the present paper was being prepared, an abstract appeared (Raviola, Goodenough & Raviola, 1978) describing what was suggested to be the native structure of nexuses. According to this report, the application of a rapid freezing technique avoiding chemical fixation and cryoprotectants revealed a nexus structure slightly different from that usually found in chemically fixed tissue[1]. Unfortunately, this technique of rapid freezing seems to be unsuitable for application to Purkinje fibers, since the connective tissue surrounding the muscle cells is thicker than the surface layer which is vitrified by this technique. Also, dissection of the muscle would presumably result in only a vitrification of a layer of injured cells. Thus, the results obtained with chemically fixed material have to be regarded with caution. However, the differences in morphology of coupled and uncoupled cells shown in the present work nevertheless indicate structural changes of nexus in response to uncoupling procedures.

We are grateful to Prof. W. Simon for his generous gift of the calcium carrier. We thank Ms. M. Honnecker, Mrs. I. Kuemmel, and Mr. R. Weiss for excellent technical assistance, Ms. M. Bosch for preparation of the typescript, and Dr. S. Socolar for his constructive review of the manuscript. This work was supported by the Deutsche Forschungsgemeinschaft, Sonderforschungsbereich 38 "Membranforschung".

References

Adrian, R.H., Chandler, W.R., Hodgkin, A.L. 1970. Voltage clamp experiments in striated muscle fibers. *J. Physiol. (London)* **208**:607

Asada, Y., Bennett, M.V.L. 1971. Experimental alteration of coupling resistance at an electronic synapse. *J. Cell Biol.* **49**:159

Ashraf, M., Halverson, C. 1978. Ultrastructural modifications of nexuses (gap junctions) during early myocardial ischemia. *J. Mol. Cell. Cardiol.* **10**:263

Barr, L., Dewey, M.M., Berger, W. 1965. Propagation of action potentials and the studies of the nexus in cardiac muscle. *J. Gen. Physiol.* **48**:797

Bates, R.G. 1973. Ion activity scales for use with selective ion-sensitive electrodes. *Pure Appl. Chem.* **36**:407

Bennett, M.V.L. 1973. Function of electric junctions in embryonic and adult tissue. *Fed. Proc.* **32**:66

Blaustein, M.P. 1974. The interrelationship between sodium and calcium fluxes across cell membranes. *Rev. Physiol. Biochem. Pharmacol.* **70**:33

Branton, D., Bullivant, S., Gilula, N., Karnovsky, M., Moor, H., Muehlethaler, K., Northcote, N., Packer, L., Satir, B., Satir, P., Speth, V., Weinstein, R. 1975. Freeze-etching nomenclature. *Science* **190**:54

Caesar, R., Edwards, G.A., Ruska, H. 1958. Electron micrsoscopy of the impulse conducting system of the sheep heart. *Z. Zellforsch. Mikrosk. Anat.* **48**:698

Caspar, D.L.D., Goodenough, D.A., Makowski, L., Phillips, W.C. 1977. Gap junction structures: I. Correlated electron microscopy and x-ray diffraction. *J. Cell. Biol.* **74**:605

Deltmer, J.W., Ellis, D. 1978. The intracellular sodium activity of cardiac Purkinje fibres during inhibition and reactivation of the Na-K pump. *J. Physiol. (London)* **284**:241

Délèze, J. 1970. The recovery of resting potential and input resistance in sheep heart injured by knife or laser. *J. Physiol. (London)* **208**:547

DeMello, W.C. 1975. Effect of intracellular injection of calcium and strontium on cell communication in heart. *J. Physiol. (London)* **25**:231

Dewey, M.M., Barr, L. 1962. Intercellular connection between smooth muscle cells: The nexus. *Science* **137**:670

Ferrier, G.R., Saunders, J.H., Mendez, C. 1973. A cellular mechanism for the generation of ventricular arrhythmias by acetylstrophanthidin. *Circul. Res.* **32**:600

Flagg-Newton, J., Loewenstein, W.R. 1979. Experimental depression of junctional membrane permeability in mammalian cell culture. A study with tracer molecules in the 300 to 800 dalton range. *J. Membrane Biol.* **50**:65

Furshpan, E.F., Potter, D.D. 1968. Low resistance junctions between cells in embryos and tissue culture. *Curr. Top. Dev. Biol.* **3**:95

Gilula, N.B., Epstein, M.L. 1976. Cell-to-cell communication, gap junctions and calcium. *Symp Soc. Exp. Biol.* **30**:257

Isenberg, G. 1977. Cardiac Purkinje fibers: Resting, action and pacemaker potential under the influence of $[Ca^{2+}]_i$ modified by intracellular-injection technique. *Pfluegers Arch.* **371**:51

Isenberg, G. 1979. Risk and advantage of using strongly bevelled microelectrodes for electrophysiological studies in cardiac Purkinje fibers. *Pfluegers Arch.* **380**:91

Isenberg, G., Trautwein, W. 1974. The effect of dihydro-ouabain and lithium ions on the outward current in cardiac Purkinje fibers. Evidence for electrogenicity of active transport. *Pfluegers Arch.* **350**:41

Isenberg, G., Dahl, G. 1978. Ultrastructural changes of the gap junction correlated with increased longitudinal resistance (Purkinje fibre). *Pfluegers Arch.* **373**:R8

Jack, J.J.B., Noble, D., Tsien, R.W. 1975. Electrical Current Flow in Excitable Cells. Clarendon Press, Oxford

Langer, G.A., Serena, S.D. 1970. Effects of strophanthidin upon contraction and ionic exchange in rabbit ventricular myocardium: Relation to control of active state. *J. Mol. Cell. Cardiol.* **1**:65

[1] Unpublished experiments with quick freezing techniques in the laboratory of one of the authors recently have shown that cultured heart and liver cells exhibit a nexus structure closely resembling that described in this paper.

Loewenstein, W.R. 1966. Permeability of membrane junctions. *Ann. N.Y. Acad. Sci.* **137**:441

Loewenstein, W.R. 1967. Cell surface membranes in close contact. Role of calcium and magnesium ions. *J. Colloid Interface Sci.* **25**:34

Loewenstein, W.R. 1975. Permeable junctions. Cold Spring Harbor Symp. Quant. Biol. **40**:49

Loewenstein, W.R., Kanno, Y., Socolar, S.J. 1978. Quantum jumps of conductance during formation of membrane channels at cell-cell junction. *Nature (London)* **274**:133

Lux, H.D., Neher, E. 1973. The equilibration time course of $[K]_o$ in the cat aortex. *Exp. Brain Res.* **17**:190

McCallister, L.P., Munger, B.L., Neely, J.R. 1977. Electron microscopic observations and acid phosphatase activity in the ischemic rat heart. *J. Mol. Cell. Cardiol.* **9**:353

McNutt, N.S., Weinstein, R.S. 1973. Membrane ultrastructure at mammalian intercellular junctions. *Prog. Biophys. Mol. Biol.* **26**:45

Meier, P.C., Ammann, D., Osswald, H.F., Simon, W. 1977. Ion-selective electrodes in clinical chemistry. *Med. Prog. Technol.* **5**:1

Mobley, B.A., Page, E. 1972. The surface area of sheep cardiac Purkinje fibers. *J. Physiol. (London)* **220**:547

Oehme, M., Kessler, M., Simon, W. 1976. Neutral carrier Ca^{2+}-microelectrode. *Chimia* **30**:204

Pappas, G.D., Asada, Y., Bennett, M.V.L. 1971. Morphological correlates of increased coupling resistance at an electric synapse. *J. Cell Biol.* **49**:173

Peracchia, C. 1977. Gap junctions structural changes after uncoupling procedures. *J. Cell Biol.* **72**:628

Peracchia, C., Dulhunty, A.F. 1976. Low resistance junctions in crayfish structural changes with functional uncoupling. *J. Cell. Biol.* **70**:419

Politoff, A.L., Socolar, S.J., Loewenstein, W.R. 1969. Permeability of a cell membrane junction. Dependence on energy metabolism. *J. Gen. Physiol.* **53**: 498

Raviola, E., Goodenough, D.A., Raviola, G. 1978. The native structure of gap junctions rapidly frozen at 4 °K. *J. Cell Biol.* **79**:229a

Reuter, H., Seitz, N. 1968. The dependence of calcium efflux from cardiac muscle on temperature and external ion composition. *J. Physiol. (London)* **195**:451

Revel, F.P. 1968. Studies on the fine structure of intercellular junctions. Proceedings 26th Meeting of Electron Microscopy Society of America. p. 40. Claitors, Baton Rouge

Rose, B., Loewenstein, W.R. 1976. Permeability of a cell junction and the local cytoplasmic free ionized calcium concentration: A study with aequorin. *J. Membrane Biol.* **28**:87

Rose, B., Simpson, I., Loewenstein, W.R. 1977. Calcium ion produces graded changes in permeability of membrane channel in cell junction. *Nature (London)* **267**:625

Simon, W., Ammann, D., Oehme, M., Morf, W.E. 1978. Calcium sensitive electrodes. *Ann. N.Y. Acad. Sci.* **307**:52

Socolar, S.J., Loewenstein, W.R. 1979. Methods for studying transmission through permeable cell-to-cell junctions. *In:* Methods in Membrane Biology. E.D. Korn, editor. Vol. 10, pp. 121–177. Plenum, New York

Volkmer, I., Dahl, G., Raman, K., Stapenhorst, K. 1977. Cardioplegia according to Bretschneider for valve replacement: Clinical experiences and electronmicroscopical results. *Thoraxchirurgie* **25**:451

Weidmann. 1952. The electrical constants of Purkinje fibres. *J. Physiol. (London)* **118**:348

Weingart, R. 1977. The actions of ouabain on intercellular coupling and conduction velocity in mammalian ventricular muscle. *J. Physiol. (London)* **254**:341

Received 16 August 1979; revised 5 December 1979